Bridge Service Life and Impact of Maintenance Events on the Structural State Index

Bah, Abdoul S.; Zhang, Yan; Sasai, Kotaro; Conciatori, David; Chouinard, Luc; Zufferey, Nicolas; Power, Gabriel J.; Sanchez, Thomas; Chen, Xuande

How to cite

BAH, Abdoul S. et al. Bridge Service Life and Impact of Maintenance Events on the Structural State Index. In: Case studies in construction materials, 2025, p. 13. doi: 10.1016/j.cscm.2025.e04766

This publication URL: https://archive-ouverte.unige.ch/unige:189027
Publication DOI: 10.1016/j.cscm.2025.e04766

Case Studies in Construction Materials 22 (2025) e04766

Contents lists available at ScienceDirect

Case Studies in Construction Materials

journal homepage: www.elsevier.com/locate/cscm

Bridge service life and impact of maintenance events on the structural state index

Abdoul S. Bah [a], Yan Zhang [b], Kotaro Sasai [b], David Conciatori [a,f,*], Luc Chouinard [b], Nicolas Zufferey [e], Gabriel J. Power [c], Thomas Sanchez [d], Xuande Chen [g]

[a] Research Center on Concrete Infrastructure (CRIB), Dept. of Civil and Water Engineering, Université Laval, Québec Canada
[b] Centre d'Études Interuniversitaire des Structures sous Charges Extrêmes (CEISCE), Dept. of Civil Engineering and Applied Mechanics, McGill University, Montreal, Canada
[c] Research Center on Concrete Infrastructure (CRIB), Dept. of Finance, Insurance and Real Estate, Université Laval, Québec, QC G1V 0A6, Canada
[d] Laboratory of Composite Materials for Construction (LMC2 EA 7427), Lyon 1 University, Villeurbanne, France
[e] Geneva School of Economics and Management (GSEM), University of Geneva, Geneva 1211, Switzerland
[f] INSA de Strasbourg Laboratoire, ICube CNRS UMR 7357, Département Génie Civil, 24 boulevard de la Victoire - C 309, Strasbourg F-67 000, France
[g] Université du Québec à Rimouski, Département Génie Civil, Rimouski, Canada

ARTICLE INFO

Keywords:
Reinforced concrete
Durability
Prediction
Condition
Bridge

ABSTRACT

Managers of ageing structures aim to extend their service life through timely inspections and preventive maintenance. Currently, planning and decisions on maintenance activities are based on condition assessment methods that rely primarily on visual inspections. However, experience indicates that the deterioration is already in an advanced state at the appearance of the first visual signs of distress and precludes timely preventive maintenance interventions. In addition, the analysis of a sequence of ratings solely based on the evolution of visually based ratings provides very little insight on the rate of the deterioration, and the estimation of residual service life. The objective of this paper is to propose a procedure that supplements visual inspection reports based on structure specific nonlinear simulations of deteriorations associated with the ingress of chloride ions, corrosion of the reinforcing steel, and the cracking and spalling of concrete. Structure-specific simulations are obtained though a model that uses site-specific hourly historical meteorological data, and concrete properties from non-destructive permeability and resistivity measurements. The model is used to estimate the time to the initiation of corrosion as well as the time to the first corrosion-induced cracks to anticipate and evaluate pre-visual conditions. The proposed methodology is demonstrated for an ageing structure in Montreal (Canada). The results show that visual inspections fail in detecting the onset of corrosion for preventive maintenance, and result in prematurely deficient structures. Model simulations suggest that preventive maintenance on the bridge at year 20, corresponding to the bifurcation point of accelerated deterioration rates, would have been optimal.

* Corresponding author at: Research Center on Concrete Infrastructure (CRIB), Dept. of Civil and Water Engineering, Université Laval, Québec Canada.

E-mail addresses: david.conciatori@insa-strasbourg.fr (D. Conciatori), n.zufferey@unige.ch (N. Zufferey), gabriel.power@fsa.ulaval.ca (G.J. Power), thomas.sanchez@univ-lyon1.fr (T. Sanchez), xuande_chen@uqar.ca (X. Chen).

https://doi.org/10.1016/j.cscm.2025.e04766
Received 15 January 2024; Received in revised form 27 April 2025; Accepted 10 May 2025
Available online 12 May 2025

1. Introduction

The durability of concrete structures in North America is closely associated to climatic and environmental conditions and the need to maintain road safety during winter periods with de-icing salts (NaCl, $MgCl_2$ and $CaCl_2$). Chlorides in de-icing salts are highly corrosive and lead to a rapid degradation of the road network infrastructure [65]. The chlorides migrate into the concrete cover, destroy the passive oxide layer that protects the reinforcing steel and exposes the reinforcing steel to corrosion [36,76], which can significantly reduce the service life of structures [10,43]. Most bridges in North America were built between 1950 and 1975, resulting in a large cohort of bridges between 47 and 72 years of service [48].

Older bridges in North America are assumed to have been designed for a service life of approximately 50 years. Currently 42 % of the 617,084 US highway bridges are over 50 years old and 12 % are over 80 years old, and require major rehabilitation or replacement [5].

In 2018, Canada numbered 51,717 publicly owned bridges, Ontario having the most (15534), followed by Alberta (9400). A quarter of the bridges on local roads and rural highways were over 50 years old, with 16 % of bridges on local roads and 14 % of bridges on rural highways in poor or very poor condition [67].

For these ageing concrete structures, it is essential that maintenance and rehabilitation strategies are planned appropriately. Over the last decade, there has been increasing interest in bridge condition assessment and residual life prediction models. These models are used to develop optimal maintenance and replacement policies to extend the service life and to optimise the allocation of financial and technical resources [35,52,58,80]. For ageing structures, non-destructive testing methods are available for assessing the degree of corrosion of the reinforcing steel [14,47,69]. These measurements are used to estimate in a proactive (rather than reactive) way, the deterioration of a bridge during its life cycle. Managers aim to inspect and maintain the infrastructure while minimizing traffic interruptions or impairments [8,13,45,81].

Most deterioration prediction models in bridge management systems are derived from inspection records and derived condition states. Popular methods for this purpose include Markov chain models and Bayesian belief networks using transition or conditional probabilities [28,63]. Engineers have relied on these records but several limitations of these data have been identified [40]. Visual inspection provide only information on visible defects and the ratings are subjective and influenced by the bias of individual inspectors, which can result in erroneous condition assessments [2,39]. Previous research on condition ratings from inspections focussed on methods to analyse and predict visually-based condition ratings [77,60], and more recently by using machine learning and deep learning for the prediction of condition states of individual bridges [62,41], and for optimizing interventions at the network level [50,51]. These methods are fitted to historical data bases on visually-based condition ratings and would not improve the prediction for the initiation of corrosion. A recent review article on condition rating of bridges [30] highlights these shortcomings and suggests that future improvements should incorporate both physically-based models, and structure-specific inputs from non-destructive testing. The proposed method addresses both avenues, and a means to improve current condition rating systems.

A Markov chain is typically used to define transition probabilities for states defined by the classification system (usually 4–5 classes) for time steps corresponding to the statutory frequency of inspections (1–5 years) [46]. The Markov process assumes that the future condition state depends only on the present state and not on the past history of condition states [56]. For example, in Switzerland, deterioration curves were established from the damage inventory obtained according to the type of structure, the age, the material, and the type of element [49]. The model does not consider the physicochemical phenomena of internal deterioration or the properties of the materials. Therefore, the approach is purely statistical and dependant of the classification of structures or structural components into homogeneous classes.

Several models for the transport of chloride ions and the corrosion of reinforcing steel have been proposed in the literature. Most consider simplified climatic and environmental exposure conditions and do not consider the effect of capillarity in the presence of liquid water [22] or the multi-ionic actions [18,72]. When probabilistic approaches are implemented with Monte Carlo simulation, the models are typically even more simplified [44,64]. It has been shown that these simplified models are applicable only to idealized cases and may lead to erroneous results in real applications [42,54], it is for all of these reasons that TransChlor® model was used in this application. In addition to laboratory validation, this model has been used for detailed analyses by Steel Swiss AG [22], the Swiss highway authority (canton of Vaud), and the ETH team to assess degradation pathologies, specifically in tunnel entrances in Switzerland [15]. Current work includes simulations for the Champlain Bridge in Canada by Jacques Cartier and Champlain Bridges Incorporated (PJCCI).

The objective of this paper is to propose a procedure that supplements visual inspection reports based on structure specific nonlinear simulations of deteriorations associated with the ingress of chloride ions with TransChlor®, corrosion of the reinforcing steel, and the cracking and spalling of concrete. Structure-specific simulations, starting from the initial date of construction, are obtained though a model that uses site-specific hourly historical meteorological data and concrete properties from non-destructive permeability and resistivity measurements. The model is used to estimate the time to the initiation of corrosion as well as the time to the first corrosion-induced cracks to anticipate and evaluate pre-visual conditions. Condition states based on the degree of corrosion are used to predict the structure residual life.

The proposed model is first described, followed by its demonstration for an existing bridge in Montreal, Canada. The description of the bridge and the methodology are described in 2. The simulation of condition states of various structural elements was performed using historical climatic data, and the element-specific exposure conditions (direct, splash or mist) are described in 3. The condition states for the components are combined through a hierarchical event tree to obtain the condition state at the level of the entire structure (3.1). The influence of repairs on the component and structural condition states are evaluated in 3.2 and the condition ratings based on visual inspection and results from non-destructive tests are described in 3.3. The results demonstrate that a comprehensive

description of environmental exposure and exposure conditions of structural elements can accurately predict the early stages of degradation of structures, and can enable proactive preventive maintenance.

2. Methodology for assessing the bridge condition state

The bridge used for the demonstration of the methodology was built in 1959 in Montreal and consists of a symmetrical two-span portico (the free span is 11.4 m). The deck is a thick slab with a thickness of 1 m at the supports and 0.6 m at its centre. The side supports and the central pier are continuous across the entire width of the structure (Fig. 1). Data on the concrete was obtained from in-situ non-destructive tests.

2.1. Deterioration model

The evaluation of the condition state of components is obtained using a deterioration model that considers the hourly microclimate and environmental exposures as boundary conditions [22]. The boundary conditions of the model comprise precipitation, solar radiation, air temperature, and relative humidity. For the demonstration structure, historical climatic data is obtained from the Dorval Airport weather station at a distance of 15 km from the structure [8]. The environmental exposure consists of the presence of de-icing salts on the road surface. The contact time of salt with structural elements considers the frequency of de-icing trucks triggered by climatic conditions (rain/snowfall or high relative humidity below a threshold temperature, snowfall) and local spreading protocols (time interval between salt-spreading truck passages and volume per m^2) (Fig. 2).

The presence of water or humidity at the surface of elements is essential to the penetration of chloride ions in the concrete elements. Chloride migration into concrete is accelerated in the presence of water due to capillary suction and chloride advection by water. Consequently, liquid water contact time is the dominant factor in chloride migration, which varies as a function of the type of exposure. For direct exposure, liquid water contact time is defined as periods of precipitation, which is extended to overnight periods when precipitation occurs after sunset. For splash exposure, the water contact is assumed to start one hour after the start of precipitation and end simultaneously with the end of precipitation. Finally, for salt-laden mist exposure, there is no contact with liquid water and the water content in concrete pores is in equilibrium with the relative humidity of air [21]. Chloride transport parameters of concrete depend on its permeability [24,23]. Air permeability and electrical resistivity, obtained through non-destructive tests, provide the properties of these parameters for different structural elements of the bridge (slab, front wall and retaining walls) [8].

A database compiled by Conciatori et al., [23] is used to define concrete properties for covers classified as either low, moderate, or high permeability. These properties include the water-cement ratio (W/C), the water vapor diffusion coefficient D_h, the transport coefficient of liquid water by capillarity D_{cap} and the diffusion coefficient of chloride ions D_{Cl} [8].

The uncertainties in material properties are propagated in the TransChlor model by using the Rosenblueth point estimation method for the conditional mean and variance of the chloride content as a function of time and depth, which is assumed to follow a lognormal distribution [20]. The conditional probability of corrosion initiation as a function of time at the level of the reinforcing steel is calculated by convolution between the conditional distribution of chloride content and the (lognormal) distribution for the resistance of the steel to corrosion.

Two models are proposed. Model 1 evaluates the serviceability of the structure by quantifying the state of the material with a material index m_i. The material index is currently evaluated qualitatively by the Ministry of Transport [55] from visual inspections reports. A detailed physically-based model [8] is proposed as an alternative to objectively estimate this index from the results of the TransChlor ion transport model, which can predict more accurately the early stages of material deterioration prior to noticing visual observations of internal deteriorations. Model 2 assesses the safety of the structure against structural deteriorations such as delamination and spalling due to corrosion of the reinforcing steel. The model considers the various stages for delamination and spalling: depassivation, loss of cross-sectional area due to corrosion, expansion of corrosion products, cracking and delamination of the concrete cover. This model is used to improve the second parameter currently used by the Ministry of Transport, the behavior index b_i which rates the severity of observed physical distresses (e.g. width and length of cracks among others). The models that are proposed are general and can be extended to visually-based rating systems used by other agencies (e.g. [31,32,33]).

2.2. Model 1: evaluation of service life

The condition of a structural element is first evaluated for structural serviceability by using the probability of initiation of

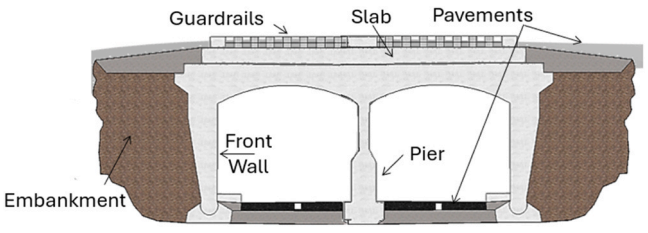

Fig. 1. Profile of the bridge (city of Montreal).

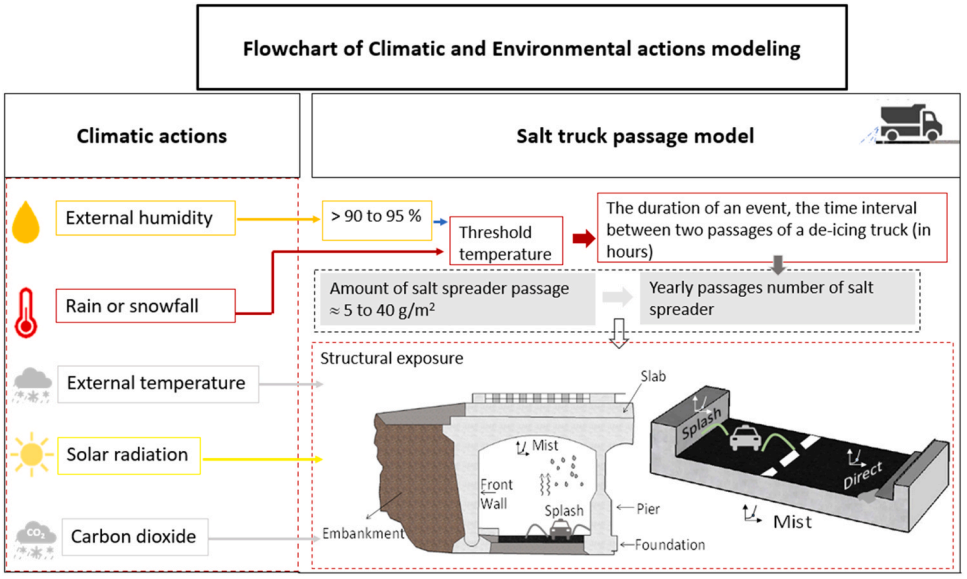

Fig. 2. Modeling of climatic and environmental actions and the passage of de-icing trucks in TransChlor®.

corrosion. To complement the visual inspection index, the state (m_i) of each element (i) is then combined considering the vulnerability of each element with a decision tree analysis to obtain the serviceability (I_M) index for the entire structure. This model 1 is described in detail in [8]. The evolution of structural deterioration in time is typically characterized by a bifurcation point that corresponds to a transition from a slow rate of deterioration to a rapid rate of deterioration, which can be estimated with the proposed methodology [25]. This point is highlighted in the Tutti diagram (Fig. 3), which corresponds to the time of corrosion initiation. The bifurcation point in time is critical for timing preventive maintenance and occurs at a level of deterioration when visual signs are not observable. In this study, the bifurcation point is assumed to correspond to the time of initiation of corrosion (T_i), which is estimated probabilistically [8].

In the management of a network of structures, the scheduling of interventions or surveillance has important financial implications and the number of interventions options becomes considerable [34,57] even for a moderately large network. A management policy is often necessary in order to reduce the number of feasible scenarios to investigate [1,3].

2.3. *Model 2: evaluating service life to ultimate limit state*

The depassivation of the surface layer of the reinforcing steel results in the corrosion of the steel in concrete structures [37,61,75]. The corrosion of the reinforcement produces corrosion products (i.e., rust) and a reduction of the cross-sectional area of steel. The volume of rust is expansive and causes pressure on the concrete, which eventually cracks and spalls [9,11]. The bond between concrete and reinforcement is also compromised resulting in a reduction of the strength and ductility of the reinforced concrete element [4,16,79].

The accurate estimation of the corrosion rate is difficult since it depends on the amount of oxygen and moisture available, which are

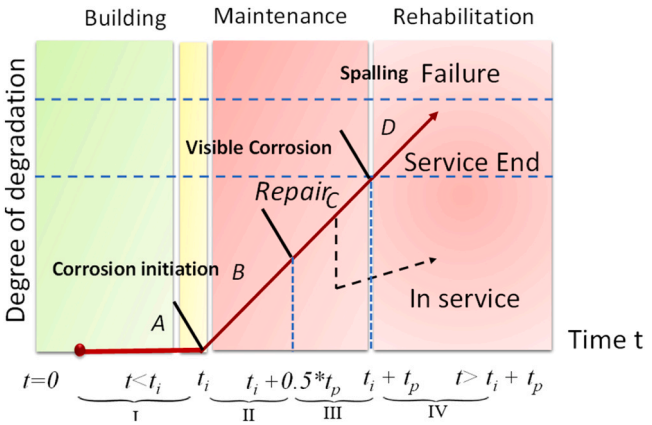

Fig. 3. Definition of condition states of a reinforced concrete bridge.

both highly variable. Prediction models based on molecular equations that convert the rate of oxygen diffusion to steel corrosion rates have been proposed [74]. However, the corrosion current density obtained from experiments or field measurements are considered to provide the most accurate estimates of corrosion rates [68]. In this research, a simple model for the corrosion rate as a function of ambient temperature is used [29].

$$J_r(t) = J_{r,20}[1 + K_c(T(t) - 20)] \quad (1)$$

where $J_{r,20}$ is the corrosion rate at 20°C, T(t) is the temperature at time t (in °C), and K_c is a factor that depends on the temperature ($K_c = 0.025$ if $T(t) < 20$°C, $K_c = 0.073$ if $T(t) > 20$°C and $K_c = 0$ if $T(t) < -20$°C). Other more comprehensive models can be used for the rate of corrosion, which consider the moisture in the concrete pores, the chloride concentration, temperature, etc. (e.g. ISO 9223 1992 [E]. Corrosion of Metals and Alloys. Classification of Corrosivity of Atmospheres). However, for the purpose of assessing the condition of a bridge for planning maintenance and repairs operations, the time to the initiation of corrosion is the most critical. The rate of corrosion that follows the time to initiation of corrosion is typically faster, and is considered an advanced stage of deterioration. The objective of the proposed rating system is to put the emphasis on intervention as early as possible to minimize the extent of repairs required.

Simplified models for corrosion-induced delamination and spalling of the concrete cover were proposed by Bazant [12] and Lounis and Daigle [53]. Once an internal crack has propagated through the depth of the concrete cover, the stresses resulting from corrosion products are assumed to remain constant until the cover delaminates or spalls off. Lounis and Daigle [53] propose the following equation for the time from corrosion initiation to the start of spalling (i.e., propagation corrosion time related to spalling):

$$t_p(sp) = \frac{\pi}{2Sj_r\left[\frac{1}{\rho_r} - \frac{\alpha}{\rho_s}\right]}\left[1 + \nu + \frac{d^2}{2c(c+d)}\right]\frac{(2cd + d^2)f_t'}{E_c} \quad (2)$$

where S is the spacing of reinforcing steek; ρ_r is the density of corrosion products (assumed at 3600 kg/m^3 for $Fe(OH)_3$; ρ_s is the density of steel (7860 kg/m^3); α is the molecular weight ratio of metal iron to the corrosion product (assumed at 0.52); and j_r is the corrosion production rate per unit area (0.8 μA/cm^2) [12].

This model is used to relate changes in the diameter of steel rebars to corrosion-induced damage limit states [52]. The random variables that are considered in the model are the spacing or the reinforcement and the thickness of the concrete cover, which are assumed to be lognormally distributed (Table 1). In this study, the total time for the onset of spalling is defined as:

$$T_t = T_i + T_p \quad (3)$$

where T_i is the corrosion initiation time, and T_p the propagation of corrosion time up to spalling. The cumulative distribution function of T_t is obtained from,

$$F_{T_t}(t_t) = P[(t_i + t_p) < t] = \int_0^{t_t} f_{T_p}(t_p)\int_0^{t_t - t_p} f_{T_i}(t_i)dt_i dt_p = \int_0^{t_t} f_{T_p}(t_p)\cdot F_{T_i}(t_t - t_p)dt \quad (4)$$

where $f_{T_i}(t_i)$ and $f_{T_p}(t_p)$ are the probability density functions for the time to initiation of corrosion and the time for corrosion propagation, respectively.

Since the time between corrosion initiation and spalling is generally long, and crack growth models are mostly linear functions of time [80], the stages of deterioration are divided into state (I) corresponding to the beginning of the service life of the structure until the initiation of corrosion. The period between corrosion initiation and midpoint in time when concrete cover spalls is defined as state (II) corresponding to the appearance of the first cracks. The state (III) describes advanced states of corrosion preceding concrete cover spalling, and finally state (IV) corresponds to spalling of the concrete cover (Fig. 3). These four condition states correspond to the ratings used by the Ministry of Transportation of Quebec (MTQ) to classify the condition of bridge elements following a visual inspection. The probabilistic functions of the characteristic periods of these different stages are presented in Eqs. (5)-(8) [80]:

$$P_I(t) = P(t < t_i) \quad (5)$$

Table 1
Random variables of the propagation model.

Exposures	Bar spacing**		Strength***		Bar diameter (mm)	Cover thickness**, c_t		
	Mean (mm)	standard deviation (mm)	f_c (MPa)	E_C (GPa)		Mean (mm)	standard deviation (mm)	Exposure
Topside of slab	180	30	41.6	21,1	30	271*	108*	Direct
Underside of slab	180	30			30	50	10	Mist
Front wall	605	65	33.4	16.94	15	46	12	Splash

* The bitumen layer is considered, ** cover thickness was obtained from georadar, *** ten cores from the slab, and three cores from the front wall.

$$P_{II}(t) = P\left[\left(t_i + \frac{t_p}{2} > t_i\right)\right] \quad (6)$$

$$P_{III}(t) = P\left[\left(t_i + \frac{t_p}{2} \leq t < t_i + t_p\right)\right] \quad (7)$$

$$P_{IV}(t) = P\left[\left(t > t_i + t_p\right)\right] \quad (8)$$

Specific actions, maintenance or rehabilitation, are proposed as a function of the ratings $P_I(t)$ to $P_{IV}(t)$ of each structural element (Table 2) (Fig. 3). The rating A, B, C and D used by the MTQ (Transportation Ministry of Quebec) for visual inspections are respectively for intact surface, the presence of small cracks, presence of concrete spalling and disintegration of the concrete surface, and the numbers correspond to the percentage of the surface of an element in each category.

3. Determination of condition states of the bridge in Montreal

Visual inspections are the primary means to currently assess the condition state of a bridge. Resulting condition states are not reliable indicators of the initial stages of deterioration and are not good predictors of future states given the difficulty of grouping structures into homogenous groups and also due to the non-stationarity of climate and traffic conditions [21,36]. Current visual inspection assessment procedures are first applied on the demonstration bridge to determine the condition states of its components and of the overall structure. This is followed by condition states inferred from the proposed model of deterioration.

Concrete permeability or materials properties for TransChlor® model are obtained from non destructive tests. Air permeability k_T of the concrete cover is obtained with the Torrent® permeability device [70,26], whereas the electrical resistivity ρ of concrete is measured with the device of Wenner [6,20,27,38]. Measurements at different locations on the bridge are used to determine the concrete cover quality (Fig. 4). The tests were performed in the summer with an air temperature of 20°C, atmospheric humidity below 70 %, and no precipitation in the days preceding the test and indicate that the concrete cover is mostly of low quality.

Simulations with TranChlor® used boundary conditions of Fig. 2, and materials properties of Fig. 4. A comparison of simulation results to chloride concentration profiles from cores from the underside and topside of the slab show good agreement (Fig. 5). The simulation results are obtained from predictions based solely on meteorological data (exposure), and material properties inferred from non-destructive tests, and are not adjusted to match observed profiles [42,54]. As reported in ACI Manual of Practice, 1989 edition Guide of concrete bridge (ACI 546.1 R), studies performed by the US Federal Highway Administration (FHWA) indicate that in the presence of moisture and oxygen, rebar corrosion is initiated at a soluble chloride content of 0.025–0.030 % of the weight of the concrete, as shown by a dash line in Fig. 5.

3.1. Model 1: evolution of the local material index (m_i) and global material index (IM)

The model simulations suggest that the best time for major preventive slab repairs should have occurred at year 12 corresponding to the bifurcation point of accelerated deterioration rates (Fig. 6). For the front wall exposed to splashing, the model suggests that an early intervention at year 8 would be optimal [8]. Management policies based solely on visual inspections favor rehabilitations when degradation has extended well beyond the bifurcation point. With the prediction of the model, a rehabilitation of the slab could have been anticipated because the internal damage at 20 years was already significant, although not visible to the naked eye (Fig. 6a). These results show that visual inspection does not provide the means to anticipate a repair and may result in a structurally deficient state of the structure.

From the state indices for each element, the overall index of the structure can be evaluated by considering the impact of the failure of the elements with an event tree presented in [8]. Fig. 6b shows the model simulation of the evolution of the material IM (serviceability) condition index of the structure without repairs. The structural condition index indicates a rapid rate of deterioration early in the service life of the abutments walls and piers in the splash zones due to capillary suction [19,24,66].

The model simulations indicate a rapid degradation of the front walls and abutments at year 8. To maintain a high rating, minor work on the front walls and abutments and the lower portions of the piers could have been performed. After 8 years, the overall deterioration rate slows down, and the serviceability and safety indexes stabilize up to year 18 (Fig. 6). Starting at year 18, the front wall has reached the lower limit of the indices, resulting in a phase between about years 20 and 35 when the slab deteriorates at a slower rate. From year 35 onwards, the rate of deterioration of the slab is slower. At year 45, the overall ratings are approaching the $P_{III}(t)$-rating zone. This corresponds to the beginning of detachment of concrete fragments from under the slab (Model 2 in the next section) (Fig. 9b) that has motivated the managers to intervene on the structure. Degradation to the $P_{III}(t)$-rating occurs at around year

Table 2
City of Montreal Asset Management Criteria [73].

Ratings	Condition index m_i of the structure (%)	Descriptions
A	≥ 75	No intervention required
B	> 40 and < 75	Requiring repairs
C	≥ 30 and ≤ 40	Requiring major repairs
D	< 30	Requiring replacement

Quality of the concrete cover	Index
Highly permeable	5
Permeable	4
Medium permeability	3
Low permeability	2
Very low permeability	1

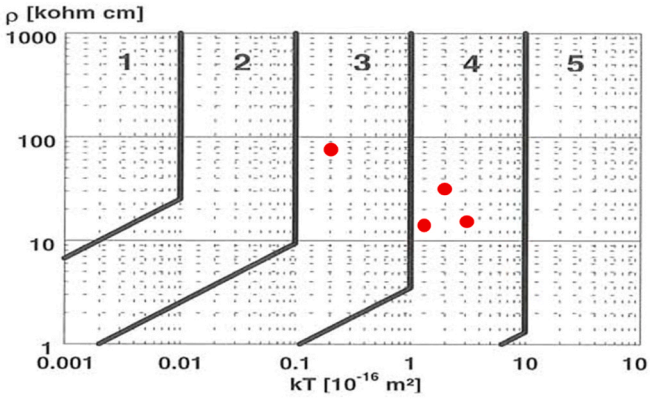

Fig. 4. Concrete quality (1−5) according to the air permeability and resistivity measurements [70].

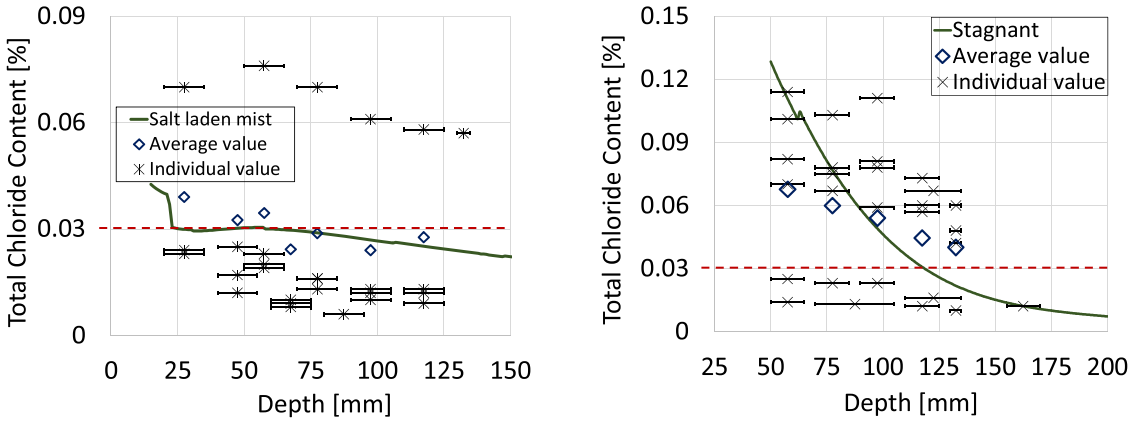

Fig. 5. Total chloride ion content (% concrete mass) for core samples from the bridge in Montreal and predictions from TransChlor®. Left part: slab underside. Right part: slab topside. The red line defines the threshold chloride content for the initiation of corrosion.

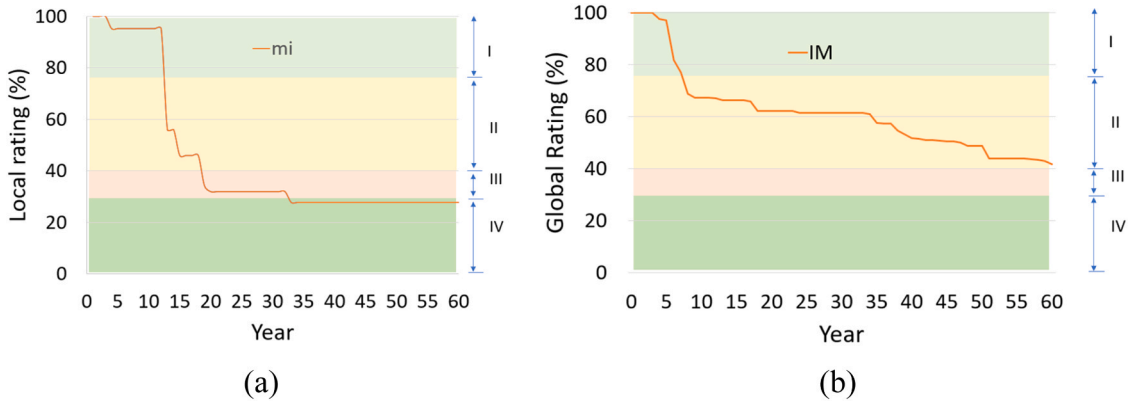

Fig. 6. Evolution of the state condition (a) of the material index (m_i) of the bridge front wall; (b) Material Index (IM) of the structure.

60.

At year 45, the level of degradation is high and visible on the surface of the concrete cover [7,17,78]. To improve the condition of structures, corrective and preventive repair strategies are required [59,71]. An example of preventive repair of a major structural element and its effect in improving the overall structural performance is demonstrated next for the slab.

3.2. Model 1: influence of slab repair

The model can be used to simulate the effect of repairs at different times during the service life. For example, if a repair is done at year 51 by partially demolishing the concrete cover and repairing with new concrete on the top of the slab, and with shotcrete for its underside. The top and bottom slab repairs were modeled, and the concentration profiles of total chloride ions before and after the slab repair are presented in Fig. 7. The model considers a demolition of the concrete cover of 50 mm at the underside of the slab and 78 mm at the topside of the slab The threshold limit for corrosion initiation is between 0.025 % and 0.03 % by mass of concrete. These profiles indicate that following the repair, the chloride front again reaches the corrosion threshold 21 years after the repair.

The influence of this repair also has an impact on the overall index of the structure. The pre-repair and post-repair material indices (i.e.: IM, IM (Repair), are shown in Fig. 8. The slab is a main element of the structure, after its repair, the overall condition index ratings is improved by 13.50 % for the material condition IM of the structure and remains in the state II.

3.3. Model 2: visual Inspections and predictions model

The historical ratings from inspection reports for the demonstration bridge are summarized in Table 3 and illustrated in Fig. 9. Vertical lines in Fig. 9 indicate the times (45 and 58 years) at which rehabilitation was done to the front wall, the underside and the topside of the slab.

The modeling of the bridge shows significant deterioration of the slab (Fig. 9a and Fig. 9b) after of 35 years of service. Curve $P_I(t)$ shows the probability of corrosion initiation: the bifurcation point for the top of the slab, is within the first 10 years of service (Fig. 9a), while for the underside of the slab with mist exposure, it is around 20 years of service (Fig. 9b) due to the high relative humidity and concrete porosity. Capillary suction contributes to a faster deterioration rate in the splash zone (Fig. 9c) with corrosion initiation after 5 years of service life. The model indicates that the slab reaches an advanced state of degradation with the development of cracks (curve $P_{II}(t)$) followed by spalling (curve $P_{III}(t)$) after 35 years (Fig. 9a). The effects of capillary suction and diffusion on deterioration are more rapid and significant in the splash zone and spalling and cracking (state $P_{III}(t)$) appear after 8 years followed by disintegration of the concrete cover, and exposure of the reinforcing bars (state $P_{IV}(t)$) (Fig. 9c). The high rate of deterioration observed in the splash zone is also related to the high permeability of the concrete of the structure (Fig. 4). The high concentration of chloride ions measured in the slab and visible signs of corrosion are consistent with the absence of a waterproofing membrane on the top of the slab.

Comparing the model results with visual inspection records, the following observations can be made:

1. At 45 years of service, the internal faces of the abutment walls (splash and salt laden mist exposure) were demolished and repaired. A concrete thickness of about ten centimeters was added in the splash zones (bottom of the wall) and, above, the damaged zones were repaired with a thin layer of projected concrete. With this restoration, the condition of the front wall (Table 3) returns to $P_I(t) = 100$ % rating. Thereafter, the front wall degrades again, with the apparition of 50 % of the surface with a state $P_{II}(t)$ at 52 years, (i.e., 7 years later), and again a rehabilitation at 57 years, (i.e., 12 years later).

   The repair did not remove all chloride ions in the concrete cover after the first intervention at 45 years since the deterioration kinetics are faster 12 years after the first intervention (Table 3), due to chloride remaining in the old concrete. Thus, visual inspections have limitations since the $P_{II}(t) = 100$ % rating after the first repair should be lower due to the presence of chloride ions in the concrete cover. The model simulations show that after 20 years the wall was in very poor condition at the time of the first

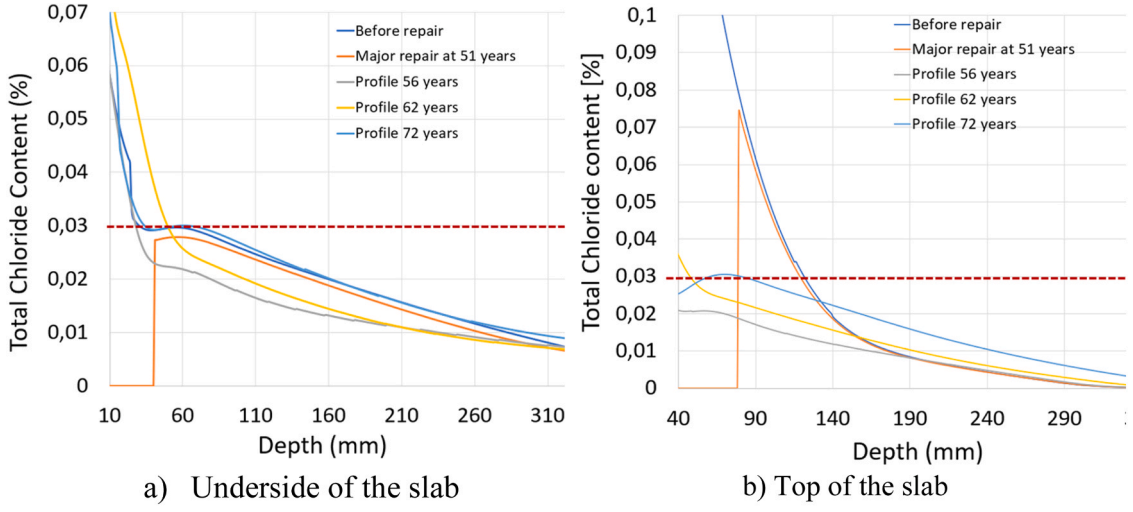

Fig. 7. Total chloride ion profile as a function of the depth before and after repair at year 51, a) underside of the slab, b) topside of the slab.

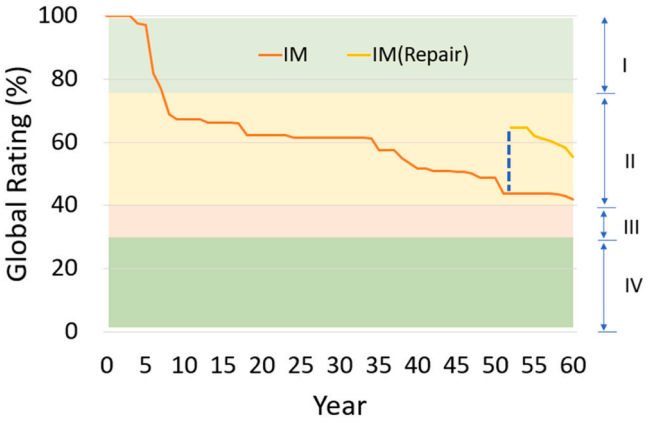

Fig. 8. Evolution of the global index of the structure before repair (IM) and after slab repair IM(Repair).

Table 3
Historical visual inspection data of the bridge under study.

Time (Year)	Visual inspection (%)											
	Front wall				Underside of the slab				Topside of the slab			
	I	II	III	IV	I	II	III	IV	I	II	III	IV
0	1	0	0	0	1	0	0	0	1	0	0	0
44	0	0	0.05	0.95	0	0.6	0.1	0.3	-	-	-	-
45	1	0	0	0	1	0	0	0	1	0	0	0
47	0.8	0.2	0	0	-	-	-	-	1	0	0	0
52	0.5	0.5	0	0	0.7	0.3	0	0	1	0	0	0
57	0.99	0	0.1	0	0.99	0.01	0	0	0.8	0.2	0	0
58	1	0	0	0	1	0	0	0	1	0	0	0

intervention with the reinforcement exposed. Specifically, it shows that the wall has a local index of $P_{IV}(t) = 95$ % before repair to $P_I(t) = 100$ % after repair at 45 years and $P_{III}(t) = 10$ % at 57 years.

2. At 45 years of service, the slab was partially demolished on its top side and repaired, without installing a waterproofing membrane. As before, the repair improved the condition of the slab to a rating of $P_I(t) = 100$ %. In contrast, the condition of the topside of the slab is not inspectable before the intervention. No deterioration is noted for the next 7 years and 5 years later, the loss is minimal with 20 % of the surface with a rating $P_I(t)$. Nonetheless, the managers repaired the slab 13 years after the first intervention by adding a waterproofing membrane (Table 3). The model simulations predict a decrease in condition rating of about 50 % at the time of the first repair. Although the condition of the topside of the slab was still in good condition, the condition of the underside has certainly motivated the managers to intervene on the whole structure. In this case, repair work on the topside of the slab could have been avoided at 57 years; however, it was more prudent to carry out this work with the addition of a waterproofing membrane to ensure greater slab durability, as good practice demanded at the time.
3. The underside of the slab was repaired with projected concrete at year 45. Before this repair, 40 % of the surface had a $P_{II}(t)$ rating, 10 % $P_{III}(t)$, and 30 % $P_{IV}(t)$ and the remaining 20 % is in good condition. After repair, the $P_I(t)$ rating is restored to 100 % of the surface. The $P_I(t)$ rating is obtained only on 30 % of the surface 7 years after the repair and second rehabilitation is carried out 5 years later to restore the $P_I(t)$ rating. The model simulations show that at the time of the first repair at year 45, 35 % of the surface has a rating of $P_{III}(t)$ and a rating $P_{IV}(t)$ expected at year 47. Again, the model showed a similar rate of degradation at 45 years as observed visually and accelerated kinetics up to 57 years. Considering this result, a repair of the entire contaminated surface would have been preferable at 45 years and would have avoided additional work at 57 years.

In the hypothetical repair in 3.2, the repair of the underside and topside of the slab was performed at year 51 (Fig. 7) to restore the underside and topside of the slab to ($P_I(t) = 100$ %). The condition of the underside of the slab was downrated to ($P_I(t) = 0.7$ %) and ($P_{II}(t) = 0.3$ %), while the topside of the slab retained a rating ($P_I(t) = 100$ %) based on a visual inspection (Table 3). This rehabilitation of the slab of the structure therefore raises the condition of the structure slightly away from the $P_{III}(t)$ rating; however, without returning to the $P_I(t)$ rating. The $P_{II}(t)$ condition is a characteristic of structures in good condition requiring additional repair work corresponding to the criteria of the Quebec infrastructure inventory (Table 2). For the structure, to recover an $P_I(t)$ rating, additional repair work is required on important elements such as the piers.

At the level of the reinforcing steel, the concentration can vary rapidly, increasing or decreasing according to fluctuating boundary conditions and the movement of water in the concrete interstices. The various probabilities are calculated on the assumption that the chloride concentration does not decrease at the level of the reinforcing steel, which explains the long durations of constant probability

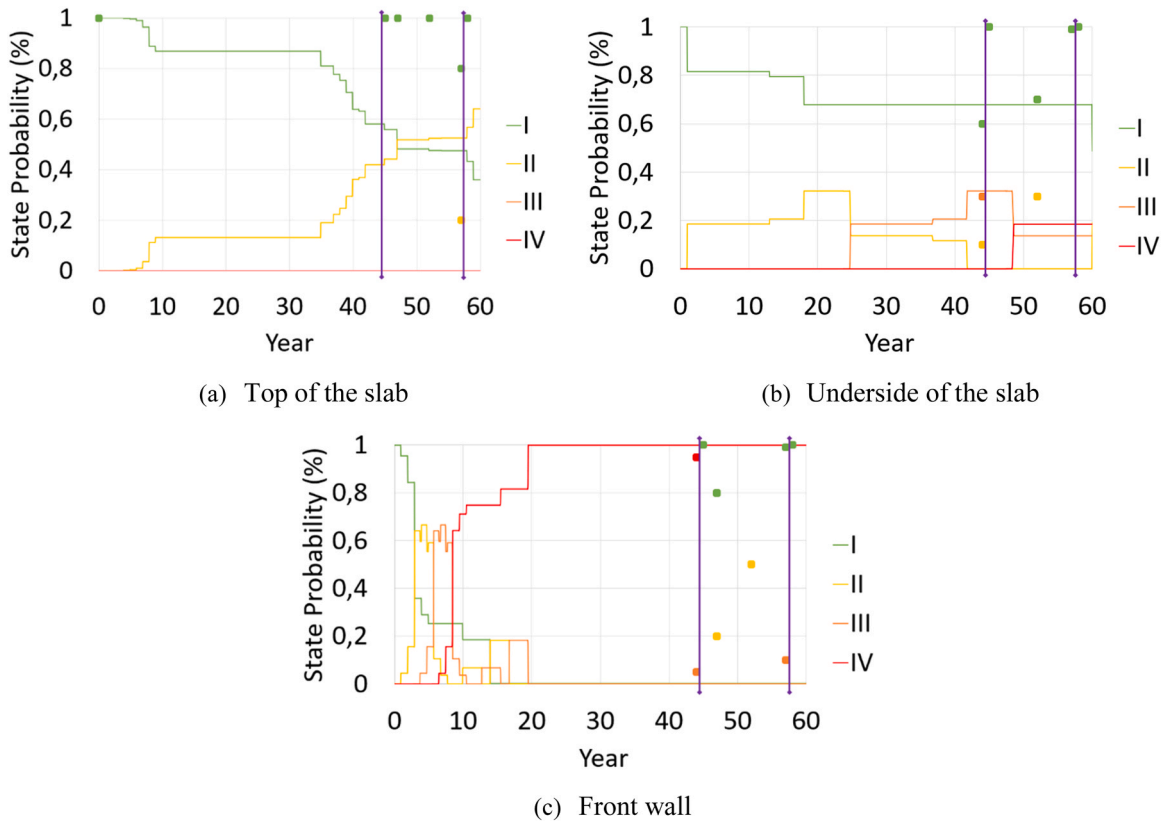

Fig. 9. Probabilities of state conditions as a function of time (observed: points; predicted: continuous line) (a) Topside of slab (direct exposure), (b) Underside of the slab (mist exposure) and (c) Front wall (splash exposure).

followed by staircase-like fluctuation in the Fig. 6.

The results of visual inspection cannot identify early degradations and may lead to a prematurely structurally deficient state of the structure. Model simulations based on the local microclimate history enable us to anticipate preventive repairs early in the service life of the structure (Fig. 3) and avoid major repairs that could have significant financial and social impacts in the middle and long term.

Conclusions

In this study, a probabilistic temporal prediction model of the serviceability and structural behaviour in a severe climatic environment was proposed. The modeling uses non-destructive evaluation to estimate material properties and a model of chloride transport depending on aging concrete structures exposed to climatic and environmental action over time. In addition to the prediction of the condition of structures, the effects of maintenance actions on the chloride transport in concrete, and their influence on the structural behaviour and serviceability of structures, were also discussed. Using the proposed modeling approach, the following conclusions can be drawn:

- The proposed methodology improves the current bridge inspection and condition assessment methodologies, which are primarily based on visual inspections. The methodology is implemented by proposing simple non-destructive permeability and resistivity tests, which provide structure-specific material information as input for a chloride-ingress model as a function of winter-time exposure. This information is essential for the early detection of the onset of corrosion and its inclusion in the rating system.
- The objective of the paper is to present the method and a detailed example for a bridge. The approach has been applied to other bridges (e.g. Champlain Bridge in Montreal) and is now mentioned in the manuscript. We would recommend that the procedure could be applied broadly to classes of structures that share similar construction practices, history and exposure. The NDT tests are easy to perform, and the model for chloride ingress can be used over large regions with similar climatology.
- For aging structures, the degradation of the structures increases more rapidly in the presence of corrosion products. The assessment of the durability of a structure can be improved with a probabilistic model coupled with non-destructive testing to detect early deterioration contrary to visual inspection. The results from the model in this case study indicates that the condition of this structure built in the 1950s was significantly degraded after 50 years. This reflects the design concept of these aging structures

which currently have an average lifespan of 60 years. The results indicate that a strategy of early intervention would have been effective din extending the service life of the structure before major interventions.

- A comparison of historical visual inspection reports with ratings derived from the proposed model, demonstrates the benefits of the latter to predict the deterioration bifurcation point for preventive maintenance. The benefits of early intervention were demonstrated by simulating the effect of early repairs instead of delaying a response until major repairs were the only remaining option.
- Given the statistics that aging structures are in poor or very poor condition in North America, it is interesting to note that the global index of the structure also allows to have a subjective idea on the extent of the degradations and thus of the works to be carried out in a global way. This index makes it possible to detect whether the structures in a network need earlier interventions.
- The methodology of this research integrates decision making from visual inspection and a prediction model. However, it is interesting to note that the choice of the model is not limitative and that the proposed method is feasible for any other type of degradation on structures and for any type of construction material used.

The strong growth of civil engineering infrastructure networks and the delayed intervention time highlight the need to consider structural safety risks at the local and the network scales.

CRediT authorship contribution statement

Power Gabriel J.: Supervision, Methodology. **Zufferey Nicolas:** Writing – review & editing, Supervision, Methodology, Formal analysis, Conceptualization. **Chen Xuande:** Investigation, Formal analysis. **Sanchez Thomas:** Writing – review & editing, Supervision, Methodology, Formal analysis, Data curation. **Zhang Yan:** Investigation, Formal analysis. **Bah Abdoul S.:** Writing – review & editing, Writing – original draft, Visualization, Validation, Software, Methodology, Investigation, Formal analysis, Data curation, Conceptualization. **Sasai Kotaro:** Investigation, Formal analysis. **Chouinard Luc:** Validation, Supervision. **Conciatori David:** Writing – review & editing, Validation, Supervision, Software, Resources, Project administration, Funding acquisition, Formal analysis, Data curation, Conceptualization.

Funding

The authors gratefully acknowledge the Islamic Development Bank, Fonds de recherche du Québec – Nature et Technologies for their financial support.

Declaration of Competing Interest

The authors declare that they have no known competing financial interests or personal relationships that could have appeared to influence the work reported in this paper.

Data Availability

Data will be made available on request.

References

[1] B.T. Adey, T. Herrmann, K. Tsafatinos, J. Lüking, N. Schindele, R. Hajdin, Methodology and base cost models to determine the total benefits of preservation interventions on road sections in Switzerland, Struct. Infrastruct. Eng. 8 (7) (2012) 639–654, https://doi.org/10.1080/15732479.2010.491119.
[2] R.S. Adhikari, O. Moselhi, A. Bagchi, Image-based retrieval of concrete crack properties for bridge inspection, Autom. Constr. 39 (2014) 180–194, https://doi.org/10/f5szzx.
[3] J.O. Almeida, P.F. Teixeira, R.M. Delgado, Life cycle cost optimisation in highway concrete bridges management, Struct. Infrastruct. Eng. 11 (10) (2015) 1263–1276, https://doi.org/10.1080/15732479.2013.845578.
[4] C.A. Apostolopoulos, V.G. Papadakis, Consequences of steel corrosion on the ductility properties of reinforcement bar, Constr. Build. Mater. 22 (12) (2008) 2316–2324, https://doi.org/10.1016/j.conbuildmat.2007.10.006.
[5] ASCE. (2021). *American Infrastructure Report Card,* ⟨https://infrastructurereportcard.org/wp-content/uploads/2020/12/Bridges-2021.pdf⟩.⟨⟩⟨https://infrastructurereportcard.org/wp-content/uploads/2020/12/Bridges-2021.pdf⟩.
[6] P. Azarsa, R. Gupta, Electrical resistivity of concrete for durability evaluation: a review, *Adv. Mater. Sci. Eng.* (2017) 1–30, https://doi.org/10/gbj76c.
[7] A.S. Bah, T. Sanchez, Y. Zhang, K. Sasai, D. Conciatori, L. Chouinard, G.J. Power, N. Zufferey, Assessing the condition of reinforced concrete bridge using visual inspection ratings, septembre 25, XV Int. Conf. Durab. Build. Mater. Compon. (DBMC 2020) (2020). https://doi.org/10/ghhpg4.
[8] A.S. Bah, T. Sanchez, Y. Zhang, K. Sasai, D. Conciatori, L. Chouinard, G.J. Power, N. Zufferey, Assess. Cond. State a Concr. Bridge Comb. Vis. Insp. Nonlinear deterio (2022) 17.
[9] I. Balafas, C.J. Burgoyne, Modeling the structural effects of rust in concrete cover, J. Eng. Mech. 137 (3) (2011) 175–185, https://doi.org/10.1061/(ASCE)EM.1943-7889.0000215.
[10] E. Bastidas-Arteaga, Reliability of reinforced concrete structures subjected to corrosion-fatigue and climate change, Int. J. Concr. Struct. Mater. 12 (1) (2018) 10, https://doi.org/10.1186/s40069-018-0235-x.
[11] A.M. Bazán, J.C. Gálvez, E. Reyes, D. Galé-Lamuela, Study of the rust penetration and circumferential stresses in reinforced concrete at early stages of an accelerated corrosion test by means of combined SEM, EDS and strain gauges, Constr. Build. Mater. 184 (2018) 655–667, https://doi.org/10.1016/j.conbuildmat.2018.06.195.
[12] Z.P. Bazant, Physical model for steel corrosion in concrete sea structures—Theory, J. Struct. Div. 105 (6) (1979) 1137–1153, https://doi.org/10.1061/JSDEAG.0005168.
[13] N. Bertola, C. Küpfer, E. Kälin, E. Brühwiler, Assessment of the environmental impacts of bridge designs Involving UHPFRC, Sustainability 13 (22) (2021) 12399, https://doi.org/10/gnm4vr.

[14] Bien et al. (2019). *Taxonomyof non-destructive field tests of bridge materials and structures,*.
[15] J. Bisschop, Y. Schiegg, F. Hunkeler, Modelling the corrosion initiation of reinforced concrete exposed to deicing salts, Conf. éR. éRatio Suisse (2016). ⟨https://books.google.ca/books?id=bYwOkAEACAAJ⟩.
[16] R. Capozucca, Damage to reinforced concrete due to reinforcement corrosion, Constr. Build. Mater. 9 (5) (1995) 295–303, https://doi.org/10.1016/0950-0618(95)00033-C.
[17] P.C. Chang, A. Flatau, S.C. Liu, Review paper: health monitoring of civil infrastructure, Struct. Health Monit. 2 (3) (2003) 257–267, https://doi.org/10.1177/1475921703036169.
[18] X. Chen, D. Conciatori, T. Sanchez, L. Sorelli, B. Selma, C. Mohamed, Numerical modeling of multi-ionic transport with/without electrical field applied in sound and microcracked ordinary and ultra-high-performance fiber-reinforced concrete, Arch. Civ. Mech. Eng. 23 (4) (2023) 232, https://doi.org/10.1007/s43452-023-00765-w.
[19] X. Chen, T. Sanchez, D. Conciatori, H. Chaouki, L. Sorelli, B. Selma, M. Chekired, Numerical modeling of 2D hygro-thermal transport in unsaturated concrete with capillary suction, J. Build. Eng. 45 (2022) 103640 https://doi.org/10/gnm4vt.
[20] Conciatori, D. (2006). *Effet du microclimat sur l'initiation de la corrosion des aciers d'armature dans les ouvrages en béton armé* [Thèse de doctorat, École Polytechnique Fédérale de Lausanne]. ⟨http://infoscience.epfl.ch/record/56049⟩.
[21] D. Conciatori, E. Brühwiler, A.-G. Dumont, Actions microclimatique et environnementale des ouvrages d'art routiers, *Can. J. Civ. Eng.,* 36 (4) (2009) 628–638, https://doi.org/10/bsxs8q.
[22] D. Conciatori, E. Brühwiler, C. Linden, Numerical simulation of the probability of corrosion initiation of RC elements made of reinforcing steel with improved corrosion performance, Struct. Infrastruct. Eng. (2018) 1–9, https://doi.org/10/gc5scx.
[23] D. Conciatori, F. Laferrière, E. Brühwiler, Comprehensive modeling of chloride ion and water ingress into concrete considering thermal and carbonation state for real climate, Cem. Concr. Res. 40 (1) (2010) 109–118, https://doi.org/10/bd9q4n.
[24] D. Conciatori, H. Sadouki, E. Brühwiler, Capillary suction and diffusion model for chloride ingress into concrete, *Cem. Concr. Res.*, *38*(12), 1401-1408 (2008) https://doi.org/10/b3gvv4.
[25] de Sitter, W. R. (1983). Costs of service life optimization. «The Law of Fives». CEB-RILEM Workshop on Durability of Concrete Structures, Copenhagen, Denmark, May 18–20, 1983.
[26] Denarié, Emmanuel, Maître Michael, Conciatori, David, & Brühwiler, Eugen. (2005). Air permeability measurements for the assessment of the in situ permeability of cover concrete, Rehabilitation and Retrofitting. International Conference on Concrete Repair, 6 p.
[27] R. du Plooy, S. Palma Lopes, G. Villain, X. Dérobert, Development of a multi-ring resistivity cell and multi-electrode resistivity probe for investigation of cover concrete condition, NDT E Int. 54 (2013) 27–36, https://doi.org/10/f4pwpw.
[28] A.C. Estes, D.M. Frangopol, Updating bridge reliability based on bridge management systems visual inspection results, J. Bridge Eng. 8 (6) (2003) 374–382, https://doi.org/10/b3k44b.
[29] EU—Brite EuRam III (2000). Duracrete—final technical report general guidelines for durability design and redesign. Technical report, Document BE95-1347/R17.
[30] N. Faris, T. Zayed, A. Fares, Review of condition rating and deterioration modeling approaches for concrete bridges, Buildings 15 (2025) 219, https://doi.org/10.3390/buildings15020219.
[31] FHWA, Traffic control systems handbook, US Department of Transportation, Federal Highway Administration, *Publ. Number.: FHWA-SA-95-032 HTA-30/5-96 (3M)EW* Febr. *1996* (1996) *dot_41949_DS1.pdf*.
[32] FHWA. (2001). Public Roads—Reliability of Visual Bridge Inspection, Issue No: Vol. 64 No. 5 March/April 2001 -. Public Roads, 6.
[33] FHWA-HRT-13-024 (2012). *Surface Resistivity Test Evaluation as an Indicator of the Chloride Permeabilityof Concrete*. ⟨https://www.fhwa.dot.gov/publications/research/infrastructure/pavements/13024/13024.pdf⟩.
[34] D.M. Frangopol, M. Liu, Maintenance and management of civil infrastructure based on condition, safety, optimization, and life-cycle cost*, Struct. Infrastruct. Eng. 3 (1) (2007) 29–41, https://doi.org/10.1080/15732470500253164.
[35] D.M. Frangopol, M. Soliman, Life-cycle of structural systems: recent achievements and future directions, Struct. Infrastruct. Eng. 12 (1) (2016) 1–20, https://doi.org/10.1080/15732479.2014.999794.
[36] K. Gode, A. Paeglitis, Concrete bridge deterioration caused by de-icing salts in high traffic volume road environment in Latvia, Balt. J. Road. Bridge Eng. 9 (3) (2014) 200–207, https://doi.org/10.3846/bjrbe.2014.25.
[37] J.A. Gonzalez, Some questions on the corrosion of steel in concrete—Part !: when, how and how much steel corrodes, Mat6riaux Et. Constr. ~Mater. Struct. 29 (1996) *40–46*, 8.
[38] K.R. Gowers, S.G. Millard, Measurement of concrete resistivity for assessment of corrosion severity of steel using wenner technique, Acids Mater. J. 96 (5) (1999) https://doi.org/10/ggr6zp.
[39] Gutkowski, R.M., & Arenella, N.D. (1998). *INVESTIGATION OF PONTIS - A BRIDGE MANAGEMENT SOFTWARE*. 43.
[40] Z. Hamida, J.-A. Goulet, State-space models for network-scale analysis of bridge inspection data, South Korea (2019) 8.
[41] J. Hong, S.,J. Jeon, Efficient Decision Tree-Based Classification Models to Predict Safety Rating for Bridge Maintenance, J. Infrastruct. Syst. 31 (1) (2025) 04024031.
[42] Y. Hosokawa, K. Yamada, B. Johannesson, L.-O. Nilsson, Development of a multi-species mass transport model for concrete with account to thermodynamic phase equilibriums, *Mater. Struct.*, *44*(9), 1577-1592 (2011) https://doi.org/10/cbcq5f.
[43] X. Hu, C.S. Poon, Chloride-related steel corrosion initiation in cement paste prepared with the incorporation of blast-furnace slag, Cem. Concr. Compos. 126 (2022) 104349, https://doi.org/10.1016/j.cemconcomp.2021.104349.
[44] Ishida. (2000). *Ishida T, Maekawa K, A computational method for performance evaluation of cementitious materials and structures under various environmental actions, Integrated Life-Cycle Design of Materials and Structures—ILCDE.pdf*.
[45] Y. Jeong, W. Kim, I. Lee, J. Lee, Bridge inspection practices and bridge management programs in China, Japan, Korea, and U.S, J. Struct. Integr. Maint. 3 (2) (2018) 126–135, https://doi.org/10.1080/24705314.2018.1461548.
[46] Y. Jiang, K.C. Sinha, Bridge service life prediction model using the Markov chain, Transp. Res. Rec. 1223.1 (1989) 24–30.
[47] S. Kashif Ur Rehman, Z. Ibrahim, S.A. Memon, M. Jameel, Nondestructive test methods for concrete bridges: A review, Constr. Build. Mater. 107 (2016) 58–86, https://doi.org/10/gfgt92.
[48] K.J. Kostuk, G.A.S. Tadros, G, Comparing conventional and innovative bridge deck options: A life cycle engineering and costing approach. Dans *Advances in Bridge Maintenance, Safety Management, and Life-Cycle Performance, Set of Book & CD-ROM*, CRC Press, 2006.
[49] Ladner, M. (1994). Systematische Auswertung von Schäden an Brücken,Bundesamt für Strassenbau, Forschungsauftrag 21/87, Rapport N°319 (VSS), Office Fédéral des Routes, Berne, 1994.
[50] L. Lai, Y. Dong, C.P. Andriotis, A. Wang, X. Lei, Synergetic-informed deep reinforcement learning for sustainable management of transportation networks with large action spaces, Autom. Constr. 160 (2025) 105302, 2024.
[51] X. Lei, Y. Dong, D.M. Frangopol, Sustainable life-cycle maintenance policymaking for network-level deteriorating bridges with a convolutional autoencoder–structured reinforcement learning agent, J. Bridge Eng. 28 (9) (2023) 04023063.
[52] Z. Lounis, T.P. McAllister, Risk-based decision making for sustainable and resilient infrastructure systems, J. Struct. Eng. 142 (9) (2016) F4016005, https://doi.org/10/f83pv7.
[53] Lounis, Z., & Daigle, L. (2008). Reliability-based decision support tool for life cycle design and management of highway bridge decks. In Annual conference of the Transportation Association of Canada (pp. 1-19).
[54] Jacques Marchand, David Conciatori, Éric Samson, Marc Gaudry, Microstructure related durability of cementitious composites: proceedings of the first international RILEM conference; [Nanjing, China, 13—15 October 2008]. Int. Conf. Microstruct. Relat. Durab. Cem. Compos. (2008) 1063–1074.

[55] MTQ. (2017). *Manuel d'entretien des structures*. ⟨http://www2.publicationsduquebec.gouv.qc.ca/dynamicSearch/telecharge.php?type= 9&file=ent-struc_2013-01_2014-01.pdf⟩.
[56] J.R. Norris, Markov Chains, Cambridge Series in Statistic and Probabilistic Mathematics, Cambridge University Press, 1998 (Cambridge University Press).
[57] A.D. Orcesi, C.F. Cremona, Optimization of maintenance strategies for the management of the national bridge stock in France, *J. Bridge Eng.*, 16 (1) (2011) 44–52, https://doi.org/10/fr8k8w.
[58] A.D. Orcesi, C.F. Cremona, Optimal maintenance strategies for bridge networks using the supply and demand approach, in: Structure & Infrastructure Engineering, 7, Taylor & Francis, 2011, pp. *765–781*, 18.
[59] A. Petcherdchoo, Probability-based sensitivity of service life of chloride-attacked concrete structures with multiple cover concrete repairs, *2018*, Adv. Civ. Eng. (2018) 1–17, https://doi.org/10.1155/2018/4525646.
[60] F. Poli, M.F. Bado, A. Verzobio, D. Zonta, Bridge structural safety assessment: a novel solution to uncertainty in the inspection practice, Struct. Infrastruct. Eng. 21 (3) (2025) 421–435, https://doi.org/10.1080/15732479.2023.2211956.
[61] A. Poursaee, Corrosion of steel in concrete structures. Dans *Corrosion of Steel in Concrete Structures*, Elsevier, 2016, pp. 19–33, https://doi.org/10.1016/B978-1-78242-381-2.00002-X.
[62] O. Qozeem, S. Abiona, H. Monique, Head, Determination of Bridge Elements Weights Using the Random Forest, Algorithm, J. Perform. Constr. Facil., 2025, 39 (1) (2025) 04024056.
[63] M.I. Rafiq, M.K. Chryssanthopoulos, S. Sathananthan, Bridge condition modelling and prediction using dynamic Bayesian belief networks, Struct. Infrastruct. Eng. 11 (1) (2015) 38–50, https://doi.org/10/gnbr3b.
[64] A.V. Saetta, et al., Analysis of chloride diffusion into partially saturated concrete, Acids Mater. J. 90 (5) (1993) *441–451 (1993)*.
[65] T. Sanchez, D. Conciatori, G.C. Keserle, Influence of the type of the de-icing salt on its diffusion properties in cementitious materials at different temperatures, Cem. Concr. Compos. 128 (2022) 104439, https://doi.org/10.1016/j.cemconcomp.2022.104439.
[66] T. Sanchez, D. Conciatori, F. Laferriere, L. Sorelli, Modelling capillary effects on the reactive transport of chloride ions in cementitious materials, Cem. Concr. Res. 131 (2020) 106033, https://doi.org/10.1016/j.cemconres.2020.106033.
[67] SC. (2018). *Statistique Canada, Enquête sur les infrastructures publiques essentielles du Canada: Actifs routiers, et actifs routiers sous forme de ponts et de tunnels, 2016*. *11*, 8.
[68] M.G. Stewart, D.V. Rosowsky, Time-dependent reliability of deteriorating reinforced concrete bridge decks, Struct. Saf. 20.1 (1998) 91–109.
[69] K. Tešić, A. Baričević, M. Serdar, Non-destructive corrosion inspection of reinforced concrete using ground-penetrating radar: a review, Materials 14 (4) (2021) 975, https://doi.org/10.3390/ma14040975.
[70] Torrent. (1997). Proceq, TORRENT Permeability Tester—Mode d'emploi, Proceq SA, Zürich.
[71] Q.C. Truong, C.-P. El Soueidy, Y. Li, E. Bastidas-Arteaga, Probability-based maintenance modeling and planning for reinforced concrete assets subjected to chloride ingress, J. Build. Eng. 54 (2022) 104675, https://doi.org/10.1016/j.jobe.2022.104675.
[72] V. Turgeon-Malette, X. Chen, A.S. Bah, D. Conciatori, T. Sanchez, M.C. Teguedy, L. Sorelli, Chloride ion permeability of Ultra-high-performance fiber-reinforced concrete under sustained load, J. Build. Eng. 66 (2023) 105842, https://doi.org/10.1016/j.jobe.2023.105842.
[73] VM. (2015). Gestion de l'actif Indice de condition générale (depuis 2015), http://ville.montreal.qc.ca/pls/portal/docs/page/transports_fr/media/documents/document_techn_indice_etat_indice_condition_generale_ICG.pdf. http://ville.montreal.qc.ca/pls/portal/docs/page/transports_fr/media/documents/document_techn_indice_etat_indice_condition_generale_ICG.pdf.
[74] K.A.T. Vu, M.G. Stewart, Structural reliability of concrete bridges including improved chloride-induced corrosion models, Struct. Saf. 22.4 (2000) 313–333.
[75] J. Warkus, M. Raupach, Numerical modelling of macrocells occurring during corrosion of steel in concrete, Mater. Corros. 59 (2) (2008) 122–130, https://doi.org/10.1002/maco.200804164.
[76] R. Wolofsky. (2011). *Corrosion Initiation of Concrete Bridge Elements Exposed to De-icing Salts—ProQuest*. ⟨https://search.proquest.com/openview/ff8f1f90d05c3a32392269308c72b12b/1?pq-origsite=gscholar&cbl= 18750&diss=y⟩.
[77] G. Xu, F. Azhari, Bridge maintenance management based on routine inspection data: a quantitative approach, J. Bridge Eng., 2025, 30(2) (2025) 04024111.
[78] I. Zambon, A. Vidovic, A. Strauss, J. Matos, J. Amado, Comparison of stochastic prediction models based on visual inspections of bridge decks, J. Civ. Eng. Manag. 23 (5) (2017). Article 5. https://doi.org/10/ggx66k.
[79] Zandi, et al., Analysis of mechanical behavior of corroded reinforced concrete structures, Acids Struct. J. 108 (5) (2011), https://doi.org/10.14359/51683210.
[80] Y. Zhang, L.E. Chouinard, D. Conciatori, Markov chain-based stochastic modeling of chloride ion transport in concrete bridges, Front. Built Environ. 4 (2018) 12, https://doi.org/10.3389/fbuil.2018.00012.
[81] Y. Zhang, L.E. Chouinard, G.J. Power, M. Tandja, D. C, J. Bastien, Flexible decision analysis procedures for optimizing the sustainability of ageing infrastructure under climate change, Sustain. Resilient Infrastruct. (2018) 1–12, https://doi.org/10/gg3w3z.